DR JUAN FORNONI (Orcid ID : 0000-0003-4116-7969)

Article type : Research Papers

Evolutionary transition between bee- and hummingbird-pollination in *Salvia*: comparing means, variances and covariances of corolla traits

Santiago Benitez-Vieyra[1], Jessica Pérez-Alquicira[2,3], Federico D. Sazatornil[1], César A. Domínguez[3], Karina Boege[3], Rubén Pérez-Ishiwara[3], Juan Fornoni[1,3,*]

[1] Instituto Multidisciplinario de Biología Vegetal, Universidad Nacional de Córdoba, CONICET, CC 495 CP 5000, Ciudad de Córdoba, Argentina.

[2] Departamento de Botánica y Zoología, CONACYT – Laboratorio Nacional de Identificación y Caracterización Vegetal, Centro Universitario de Ciencias Biológicas y Agropecuarias, Universidad de Guadalajara, Zapopan, Mexico

[3] Departamento de Ecología Evolutiva, Instituto de Ecología, Universidad Nacional Autónoma de México, 04510 Ciudad de México, México.

* Corresponding author: Juan Fornoni. Instituto de Ecologia, Universidad Nacional Autónoma de México, 04510 Ciudad de México, México.

Phone/fax: 52 55 5616 1976

email:jfornoni@iecologia.unam.mx

Running head: Covariance and trait spaces of *Salvia* flowers

This article has been accepted for publication and undergone full peer review but has not been through the copyediting, typesetting, pagination and proofreading process, which may lead to differences between this version and the Version of Record. Please cite this article as doi: 10.1111/jeb.13480
This article is protected by copyright. All rights reserved.

Accepted Article

ABSTRACT

Covariation among traits can modify the evolutionary trajectory of complex structures. This process is thought to operate at a microevolutionary scale, but its long-term effects remain controversial because trait covariation can itself evolve. Flower morphology, and particularly floral trait (co)variation, has been envisioned as the product of pollinator-mediated selection. Available evidence suggests that major changes in pollinator assemblages may affect the joint expression of floral traits and their phenotypic integration. We expect species within a monophyletic lineage sharing the same pollinator type will show not only similarity in trait means but also similar phenotypic variance-covariance structures. Here we tested this expectation using eighteen *Salvia* species pollinated either by bees or hummingbirds. Our findings indicated a non significant multivariate phylogenetic signal and a decoupling between means and variance-covariance phenotypic matrices of floral traits during the evolution to hummingbird pollination. Mean trait value analyses revealed significant differences between bee- and hummingbird-pollinated *Salvia* species while fewer differences were detected in the covariance structure between groups. Variance-covariance matrices were much more similar among bee- than hummingbird-pollinated species. This pattern is consistent with the expectation that, unlike hummingbirds, bees physically manipulate the flower, presumably exerting stronger selection pressures favouring morphological convergence among species. Overall, we conclude that the evolution of hummingbird pollination proceeded through different independent transitions. Thus, although the evolution of hummingbird pollination led to a new phenotypic optimum, the process involved the diversification of the covariance structure.

KEYWORDS: covariance space, morphospace, phenotypic integration, pollination, *Salvia*.

This article is protected by copyright. All rights reserved.

Accepted Article

INTRODUCTION

Trait correlations, arising from genetic, developmental and functional requirements, strongly affect the evolutionary trajectories of complex structures, as they may bias standing heritable variation, constraining the pathway of evolution (Maynard Smith *et al*., 1985; Schluter, 1996; Gould, 2002; Young & Badyaev, 2006; Futuyma, 2010). In this context, assessing whether or not the patterns of trait association have remained stable over evolutionary time helps us to understand the origin and evolution of complex traits (Young & Badyaev, 2006). Empirical approaches have provided mixed results. While patterns of trait association remain conserved across some large clades (e.g. Goswami 2006, Goswami *et al*., 2014, Andrade Machado *et al*., 2018), genetic correlations may change due to artificial selection in few generations (Delph *et al*. 2011), or during the first stages of adaptive radiations (Walter *et al*., 2018). Even developmental associations between size and shape may diverge among closely related species (Esquerré *et al.*, 2017; Strelin *et al*., 2018). These results suggest that evolution of trait covariances are case-specific, highlighting their dual evolutionary role both as a constraint and as an outcome of natural selection (Merilä & Björklund, 2004; Schwenk & Wagner, 2004). Trait covariation may arise from many structural and historical causes, including past selection (Gould, 2002; Merilä & Björklund, 2004; Watson *et al*., 2014; Jamniczky *et al.*, 2015). In such cases, shifts in selection regimes such as those taking place during pollinator transitions in flowering plants open a fascinating opportunity to study evolutionary changes in complex phenotypes (Wessinger & Hileman, 2016).

The hypothesis that phenotypic variances and covariances of floral traits are shaped by pollinator-mediated selection has a long history in pollination biology. Berg (1960) and Stebbins (1970) were the first to remark on the functional value of floral-trait correlations. In particular, Berg's hypothesis relies on the expectation that the morphological matching between flowers and pollinators is essential to ensure efficient pollen delivery and reception.

This article is protected by copyright. All rights reserved.

Although there has been increasing interest in the functional role of variances and covariances among functional floral traits (Pérez-Barrales *et al*., 2007; Ordano *et al*., 2008; Herrera, 2009; Murren, 2012; Armbruster *et al*., 2014; Benitez-Vieyra *et al*., 2014), we are still far from deciphering how they evolve during evolutionary transitions among pollination syndromes (Armbruster *et al*., 1999; Armbruster *et al*., 2014; Fornoni *et al*., 2016). A recent work proposed that studying the coordinated action of multiple traits represents an unexplored opportunity to better understand adaptive transitions during evolution (Fenster *et al*., 2015).

The observation that plant species that diverged from different ancestors but share similar pollinators express morphological convergence of floral traits sustains the concept of pollination syndromes (Fenster *et al*., 2004; Rosas-Guerrero *et al*., 2014; but see Reiss, 2001). For example, hummingbird-pollinated species usually have red tubular flowers, larger than those of sister species pollinated by smaller pollen vectors. Changes in pollinator assemblage may affect the variance-covariance structure of flowers, in particular the magnitude of phenotypic integration (Pérez-Barrales *et al*., 2007; Rosas-Guerrero *et al*., 2011; González *et al*., 2015; Lázaro & Santamaría, 2016). Accordingly, disintegration of correlations among traits (parcellation; Wagner & Altenberg, 1996), could allow the exploration of novel phenotypic spaces, enabling the evolution of greater phenotypic diversity.

A methodological approach to describe evolutionary changes in the floral phenotypes is to compare the species multivariate patterns of both mean trait values (i.e., morphospace *sensu* Chartier *et al*., 2014), and variance-covariance phenotypic matrices (**P**), under a phylogenetic framework. This approach allows testing whether means versus variances and covariances jointly evolved or not during transitions and reversions between bee and hummingbird pollination. After diversification, if species sharing the same pollinator group

This article is protected by copyright. All rights reserved.

Accepted Article

themselves as a cluster in both mean and variance-covariance phenotypic spaces, morphological convergence would be indicative of a functional adjustment of the phenotype during the evolutionary transition between pollination syndromes (Wessinger & Hileman, 2016). Alternatively, variance-covariance structure may remain stable or evolve by drift, expressing significant phylogenetic signal. In such case, similarity among matrices from different clades but with similar pollination syndrome is not expected.

Empirical evidence suggests that unlike hovering foraging pollinators, those that perch and physically handle flowers likely exert stronger selection pressures on floral morphology increasing the magnitude of covariation of floral traits (Pérez-Barrales *et al*., 2007; Pérez-Barrales *et al.*, 2014). While most bees must land on the flowers and have a stronger physical contact, hummingbirds are able to hover around the flower with no need of a landing platform. In accordance, we predict a significant difference in the multivariate floral phenotype between pollination syndromes, as well as a higher phenotypic similarity on both mean trait values and variance-covariance structure among melittophilous (bee-pollinated) than among ornitophilous (bird-pollinated) species across independent evolutionary transitions. In this study, means, variances and covariances of six corolla traits were analysed in bee- and hummingbird-pollinated species of Neotropical sages (*Salvia* subgenus *Calosphace*), which represent independent evolutionary transitions between melittophily and ornithophily in a monophyletic clade (Fragoso-Martínez *et al*., 2018). Data obtained from a sample of eighteen species were used to evaluate: (1) the magnitude of similarity of mean corolla traits and their variance-covariance matrices between and within bee- and hummingbird-pollinated species (following a morphospace approximation (Chartier *et al*., 2014) and Common Principal Component Analyses (Phillips & Arnold, 1999)), (2) the independent evolution of trait mean values and variance-covariance matrices, and (3) the expression of multivariate phylogenetic signal. Finally, we performed a series of numerical

This article is protected by copyright. All rights reserved.

simulations to examine the potential role of drift and selection on the observed variation of the major axes of the variance-covariance space. Drift is expected to influence the total amount of variance of a matrix (Roff, 2000; Jones *et al*., 2003), while stabilizing and correlational selection may influence phenotypic integration (Maubecin *et al.*, 2016).

MATERIAL AND METHODS

Study species and morphological measurements.

Salvia subgenus *Calosphace* is a monophyletic clade with approximately 600 species (Walker *et al*., 2004; Fragoso-Martínez *et al*., 2018). Flowers present complex bilabiate or tubular floral architectures and contrasting pollination syndromes, with most species pollinated by bees, and about one-third by hummingbirds (Wester & Claßen-Bockhoff, 2011). We sampled flowers in natural populations of 18 Mexican and South American *Salvia* species: *S. atrocyanea, S. calolophos, S. cinnabarina, S. coerulea, S. cuspidata ssp. gilliesii, S. elegans, S. fulgens, S. iodantha, S. lavanduloides, S. longispicata, S. mexicana, S. misella, S. pallida, S. personata, S. polystachya, S. purpurea, S. stachydifolia* and *S. thyrsiflora.* According to Fragoso-Martínez *et al*. (2018) bee pollination is the ancestral state in *Salvia* subgen. *Calosphace*, and multiple shifts to hummingbird pollination (and at least one reversal) have occurred. Our own ancestral state reconstruction confirms these results (see Suppl. Material and Fig. S1) and suggests that our sample includes at least two independent origins of ornithophily, while bee-pollinated species are either representatives of the ancestral state, or the product of reversals from ornithophily to melittophily. The 18 species sampled span across three of the four centres of diversity recognized by Jenks *et al*. (2013): Mexico - Central America, the Andean Region and eastern South America (Fig. S2). For each species field samples ranged between 16 and 79 plants, and 3-15 flowers per plant (Table S1). Except for *S. cuspidata, S. elegans* and *S. fulgens*, where two populations were included, one

This article is protected by copyright. All rights reserved.

Accepted Article

population per species was sampled. Harvested flowers were isolated in plastic boxes and stored within a refrigerated chamber. Flower were photographed within 10 hours of sampling. Our sample included eight species mainly pollinated by hummingbirds and ten species mainly pollinated by bees. The main pollinator guild was determined by field observations (Table S2) and previous records in the literature (Table S3). We took photographs of the side and front views of each flower using a Nikon D50 camera. Smaller flowers were photographed from closer distances to ensure flowers of different sizes occupied approximately the same relative area in the resulting photographs. In all cases we used a reference scale to transform linear measurements from pixels to millimetres, using ImageJ software (https://imagej.nih.gov/ij/). Corolla-tube length and width, corolla lower lip length and width, and corolla upper lip length and height were measured for each flower (Fig. 1). We focused on corolla traits, given that they belong to a single ontogenetic unit and because pollinator behavior strongly suggests that different corolla parts have different functions in bee and hummingbird-pollinated species (Benitez-Vieyra *et al.*, 2014). Data were log-transformed to linearize the relationships among floral traits due to allometric growth (Huxley, 1932), and to allow variances and covariances comparisons among traits and species (e.g., Lewontin, 1966). Values from the same individual plant were averaged.

Differences in mean corolla traits

Species mean values of log-transformed corolla traits were used in a phylogenetic principal component analysis (Revell, 2009) to summarize variation across the 18 selected species and to correct for nonindependence among species. Phylogeny was obtained from TreeBASE (https://treebase.org/, study S15364) and pruned to the 18 *Salvia* species. Convex hulls, the hypervolumes enclosing species coordinates, were obtained to describe the portion of the morphospace occupied by hummingbird- and bee-pollinated species. Additionally, we used

This article is protected by copyright. All rights reserved.

Accepted Article

phylogenetic generalized least squares (PGLS) to test for differences between pollination syndromes in those principal components which explained more than 5% of the total variance.

To test whether species belonging to different pollination syndromes had different flower morphology, we implemented a permutational multivariate analysis of variance (PERMANOVA, Anderson, 2001), using the *adonis* function of *vegan* R package (Oksanen *et al*., 2017). As the lack of multivariate homogeneity of variances may cause spurious significant results in this analysis, we also tested for differences in dispersion between groups. PERMANOVA does not consider the lack of independence between species due to their shared evolutionary history, thus we also used a phylogenetic MANOVA from the *geiger* R package (Harmon *et al*., 2008). However, as we obtained similar results from both methods, we only reported those from PERMANOVA (see Suppl. Routine S1). These analyses were complemented with a bootstrap procedure, randomly sampling the original data set of each species and population 1000 times to obtain an estimation of uncertainty of the multivariate combination of traits.

Differences in phenotypic variance-covariance matrices

We estimated 18 phenotypic variance-covariance matrices (**P**), one for each *Salvia* species. In the cases of *S. cuspidata*, *S. fulgens* and *S. elegans*, for which two populations were sampled, we calculated element by element weighted mean **P**-matrices (Manly, 2005). Differences between pairs of variance-covariance matrices were obtained by estimating the eigenvectors and eigenvalues of a new matrix, **C**, which specifies how to transform one matrix into the other. The matrix **C** is a multivariate analogue of the ratio between variances in univariate analyses, and results from multiplying one covariance matrix by the inverse of the other covariance matrix. From **C** eigenvalues (called relative eigenvalues) Mitteroecker &

This article is protected by copyright. All rights reserved.

Accepted Article

Bookstein (2009) derived a measure of matrix dissimilarity represented by the square root of the summed squared logarithms of the relative eigenvalues between two matrices. This metric, sometimes called Riemannian distance (Melo *et al*., 2016), is the shortest path between two matrices inside the nonlinear space of all possible covariance matrices (Mitteroecker & Bookstein, 2009), and is also invariant to all linear transformations of the original variables (Bookstein & Mitteroecker, 2014).

We obtained all pairwise Riemannian distances between the 18 *Salvia* **P**-matrices using the *MatrixDistance* function of the *evolqg* R package (Melo *et al*., 2016). Then, we performed a Principal Coordinate Analysis (PCoA, or Metric Multidimensional Scaling) using the Riemannian distance matrix (Mitteroecker & Bookstein, 2009; Bookstein & Mitteroecker, 2014, Andrade-Machado *et al*., 2018). PCoA allowed us to build a low-dimensional space where each of the original 18 **P**-matrices were represented by a single point and the Euclidean distances among them represent their similarity. PCoA was carried out using the *mmds* function of *bios2mds* R package (Pele *et al*., 2015). Within the resulting covariance space, we built convex hulls to examine whether matrices formed two groups, each corresponding to hummingbird- and bee-pollinated species, and then we tested for significant differences between pollination syndromes using a PERMANOVA and a phylogenetic MANOVA. As above, the results from both methods were similar, so we only reported those from PERMANOVA (see Suppl. Routine S1). Again, 1000 bootstrap samples were obtained for each species provided that each sample included data from at least seven individual plants to avoid rank-deficiencies and negative eigenvalues. Additionally, we used PGLS to test for differences between pollination syndromes in each principal coordinate (considering those explaining more than 5% of the total differences among **P**-matrices). To get insight about which variances and covariances better explained differences among **P**-

This article is protected by copyright. All rights reserved.

Accepted Article

matrices, we examined the correlations between the principal coordinates and the original variances and covariances between corolla traits.

To characterize matrix differences between and within pollination syndromes Common Principal Component (CPC) analyses were performed (Phillips & Arnold, 1999; Steppan, 1997; Steppan *et al.*, 2002). This analysis uses a nested hierarchy of comparisons to test hypotheses about differences among matrices, including equality (identical eigenvectors and eigenvalues, i.e. identical size, shape and orientation), proportionality (equal eigenvectors but eigenvalues differing in a scalar amount, i.e. same shape and orientation, but different sizes), all principal components in common (equal eigenvectors but different eigenvalues, i.e. same shape and orientation, non-proportional differences in size) or *i* principal components in common (*i* ranging from *n*-2 to 1, where *n* is the number of traits), and unrelated structures (matrices have dissimilar eigenvectors and eigenvalues). The best model was determined using the Akaike Information Criteria (AIC). All CPC analyses were performed with the CPC software (http://pages.uoregon.edu/pphil/software.html). We performed three CPC analyses: one using the complete set of 18 *Salvia* species, one using bee-pollinated species and one using hummingbird-pollinated species.

Phylogenetic signal

We tested for multivariate phylogenetic signal in corolla traits and those axes of the variance-covariance space that explained more than 5 % of the variation obtained from the Riemannian distance matrix. In both cases we applied K_{mult}, a generalization of Blomberg's *K* statistic for multivariate data (Adams, 2014; Goolsby, 2015), using the *Kmult* function of the *phylocurve* R package (Goolsby, 2015). Significance was assessed comparing K_{mult} with to the null distribution generated by simulation on a star phylogeny.

This article is protected by copyright. All rights reserved.

Comparison of mean trait and variance-covariance spaces

We used partial Mantel analysis (Mantel, 1967) to test for independence between differences on mean trait values and the variance-covariance structure of the flower, while simultaneously accounting for phylogenetic effects. We compared the pairwise matrix of Euclidean distances obtained from the phylogenetic principal component analysis (obtained from species mean trait values) with the pairwise matrix of Riemannian distances. Significance was assessed using the phylogenetic permutation procedure proposed by Harmon and Glor (2010) and using the 1000 bootstrap samples of matrices. Partial Mantel test has poor statistical performance, but it is the only alternative when comparing distance matrices in a phylogenetic context (Harmon & Glor, 2010, Smith *et al*., 2010).

Numerical simulations

The variance-covariance morphospace approach provides a visual inspection of **P**-matrix similarities, but it does not allow the identification of which matrix properties (size, shape and/or orientation) account for major differences across species. In contrast, CPC analysis qualitatively compares **P**-matrix properties, but it does not allow a quantitative visualization of major differences. Thus, we performed numerical simulations to explore the directions in the variance-covariance space that are associated with changes in matrix properties such as size and integration. While proportional differences between **P**-matrices have been commonly associated with the effect of drift (Roff 2000), phenotypic integration among flower traits has been claimed to be affected by differences in the history of past selection pressures (Maubecín *et al*. 2016) and pollinator assemblages (Pérez-Barrales *et al*. 2007; González *et al.* 2015). Proportional changes in matrix size were simulated by building two sets of matrices with the same eigenvectors as the original **P**-matrices, but with different size (i.e. overall variation). Thus, simulations were performed without changing the shape and

This article is protected by copyright. All rights reserved.

Accepted Article

orientation of the original **P**-matrices. Proportionality constant was set to 2 for the first run and 0.5 for the second, therefore the total amount of variance was twice the original in the first run and half in the second. These simulated matrices were projected into the original variance-covariance space using the *mmds.project* function of the *bios2mds* R package (Pele *et al*. 2012). If projected changes of species correlate with any of the major axes in the multivariate space, at least part of the variation in matrices size could be attributed to drift.

Changes in phenotypic integration were simulated following the same rationale. We projected two sets of simulated matrices into the original variance-covariance space. In the first set, the first eigenvalue accounted for 25% of the total variance, while in the second set it accounted for 85% of the total variance. Thus, we simulated two sets of matrices with the same eigenvectors (orientation) and total variance (size), but with different integration (i.e. differences in the distribution of variance among eigenvalues). Modifying the proportion of the total variance explained by the first eigenvalue is a practical way to simulate changes in phenotypic integration without altering other matrix properties (e.g. Grabowsky & Porto, 2016). Specifically, we examined differences in phenotypic integration among original and simulated matrices using the Wagner-Cheverud integration index (the relative variance of the eigenvalues from a correlation matrix: Wagner, 1984; Cheverud et al., 1989, Pavlicev et al. 2009) and the Hansen-Houle integration index (a measure related to the degree of autonomy of a character responding to directional selection when all other characters are under stabilizing selection; Hansen & Houle, 2008). Bootstrap samples were used to repeat each series of simulations 1000 times. In all cases, we found that an increase or decrease in the proportion of the total variance explained by the first eigenvalue lead to an increase or a decrease in phenotypic integration, respectively Fig. S3). A detailed description of all the procedures and an R routine is provided as supplementary material (Suppl. Routine S1).

This article is protected by copyright. All rights reserved.

Accepted Article

RESULTS

Phylogenetic principal component analysis using mean values of the original six corolla traits for each species indicated that the first two principal components explained 93.83% of the total variance (84.50% and 9.33%, respectively). Remaining principal components explained less than 5% each. The first principal component was related to corolla size. Within this axis, corolla-tube length had a strong positive loading while lower lip width and length had strong negative loadings in the second principal component (Table 1). This indicated that larger corollas have a more tubular shape. Because they are generally larger, hummingbird-pollinated species attained greater scores in the first principal component (PGLS, t = -5.239, $P < 0.001$) than bee-pollinated species. The second component, in contrast, separated species with tubular corollas from species with bilabiate corollas. PGLS also indicated significant differences between bee- and hummingbird-pollinated species in the second principal component (t = -2.436, P = 0.027). In particular, the hummingbird-pollinated *S. cinnabarina* and *S. iodantha* attained the highest scores in the second principal component, as they were characterized by long, narrow corolla tubes and very small lower lips (Fig. 2). The convex hulls of hummingbird- and bee-pollinated species (estimated from the first two principal components) did not overlap even after bootstrapping (Fig. 2, S4). As expected, PERMANOVA indicated that there were significant multivariate differences between pollination syndromes based on their mean trait values ($F_{1,16}$ = 16.828; $P < 0.0001$). We did not find significant departure from homogeneity of multivariate dispersion ($F_{1,16}$ = 1.229; P = 0.270).

In the variance-covariance space (Fig. 3), the first three principal coordinates explained 48.79% of the variance among species (21.35%, 15.16% and 12.28%, respectively). The first coordinate was negatively correlated with within-species variances in lower lip length and width and upper lip length (in all cases $|r| > 0.6$, Fig. 3). The second

This article is protected by copyright. All rights reserved.

coordinate was associated with corolla tube width variance and upper lip length – upper lip width covariance. The third coordinate was positively correlated with upper lip width variance and upper lip width – corolla tube width covariance. A full description of the first seven principal coordinates, which accounted for 80.57% of the total variance, and their correlations with traits variances and covariances can be found in Sup. Table S4. Each of these seven principal components explained more than 5% of the variation and together accounted for 80.57% of the total variance. The convex hulls of hummingbird- and bee-pollinated species (estimated from the first three principal coordinates) showed some superposition of clusters (Fig. 3). The PERMANOVA indicated that there were non-significant differences between pollination syndromes ($F_{1,16}$ = 1.268; P = 0.191). We also did not find significant departures from homogeneity of multivariate dispersions ($F_{1,16}$ = 0.043; P = 0.845). Confidence ellipsoids for P-matrices inside the variance-covariance space showed visual overlapping (Fig. S5), PERMANOVA and dispersion test results were consistently non-significant in 944 and 987 out of 1000 bootstrap samples respectively, supporting the absence of significant differences between pollination syndromes. We found significant differences only between bee- and hummingbird-pollinated species in the third and fourth principal coordinates of the covariance space (PGLS, t = 2.843, P = 0.012 and t = -2.674, P = 0.017, respectively). As multiple tests were applied to the same data set, results from PGLS have to be taken with caution.

Common Principal Components Analysis for the whole set of species revealed that **P**-matrices had an unrelated structure (Table 2), as did the comparison among hummingbird-pollinated species (Table 2). However, when comparing bee-pollinated species, CPC indicated that they shared all principal components, indicating less divergence in matrix structure (Table 2).

This article is protected by copyright. All rights reserved.

Phylogenetic signal was not significant and had similar value for the average value of floral traits (K_{mult} = 0.691, P = 0.178) and the first seven axes of the covariance space (K_{mult} = 0.611, P = 0.324). The comparison between Euclidean and Riemannian distances indicated no correlation during evolution between them (observed partial correlation r = 0.078, P = 0.108). This lack of correspondence coincides with the visual inspection of both spaces (Fig. 2 and Fig. 3), indicating the presence of two clusters related to pollination syndromes in the morphospace using trait mean values but not on the variance-covariance space. Alternative solutions obtained after bootstrapping indicated that partial correlation between spaces varied between r = -0.157 and r = 0.215 (95% confidence interval) and were consistently non significant in 867 out of 1000 bootstrap samples.

Numerical simulations

Proportional changes in matrices size showed a high correlation (r = -0.848 ± 0.0001 s.d.) with the first principal coordinate axis of the variance-covariance space (Fig. 4a). Thus, negative scores on the first principal coordinate are associated with a larger matrix size. Projecting simulated matrices revealed that changes in phenotypic integration were also associated with the first principal coordinate of the variance-covariance space, even though simulations did not result in parallel lines as above. Average vector correlation was 0.715 ± 0.078 s.d. Thus, high scores in the first principal coordinate were associated with higher phenotypic integration (Fig. 4b). Neither proportional changes in matrices size nor changes in phenotypic integration correlates with the other axes of the variance-covariance space (Table S5). Consistent results were obtained in all bootstrap samples, both for proportional changes in matrix size and integration (Fig. S6).

This article is protected by copyright. All rights reserved.

Accepted Article

DISCUSSION

In this paper, we have shown that *Salvia* species belonging to different pollinator syndromes fell into different clusters in the mean trait value analyses while no equivalent result was found for the variance-covariance space. A more detailed exploration from CPC analyses revealed that matrices from bee-pollinated species shared all eigenvectors (i.e., they shared the same orientation but differed in how variance is distributed), while **P**-matrices of hummingbird-pollinated species did not share any common axis. Thus, whereas bee-pollinated species converged morphologically through their means and the **P**-matrix structure, the evolution of hummingbird pollination was mainly accomplished by convergence in mean trait values and diversification of the variance-covariance structure of the corolla. Our simulations suggest that drift can explain part of the variation in the overall amount of variance and in phenotypic integration among **P**-matrices. The clear pattern of increment in flower size that accompanied the transition to hummingbird pollination occurred without significant convergence in the variance-covariance matrices, or a decoupling between the mean and the variance-covariance spaces.

Bee-pollinated species showed a rather similar matrix structure according to CPC analyses. Bees land on flowers during foraging and sustain, in general, stronger physical contact with flowers than hummingbirds. Thus, bee pollination requires a more specific association between corolla traits than what is likely needed for hummingbird pollination. According to ancestral state reconstruction analyses (Fragoso-Martín*ez et* al., 2018; Suppl. Material and Fig. S1), our sample of bee-pollinated species involved representatives of the ancestral state (like *S. calolophos, S. cuspidata* and *S. misella)* as well as reversals from ornithophily to melittophily (like *S. pallida, S. personata* and *S. stachydifolia*). Thus, our results suggest convergent evolution of means, variances and covariances. However, the persistence of "developmental memory", where a developmental process is primed to

This article is protected by copyright. All rights reserved.

Accepted Article

produce particular phenotypes that have been selected for in the past (Watson *et al*., 2014), should be further explored. In the case of hummingbird-pollinated species, in contrast, our results indicate convergence on mean trait values but not for the **P**-matrix structure. This lack of convergence suggests that different patterns of transition from the ancestral bee pollination syndrome occurred without altering the magnitude of the corolla phenotypic integration. Ancestral state reconstructions indicated that our sample of eight hummingbird-pollinated species involved between two and four independent transitions (Fragoso-Martínez et al., 2018; Suppl. Material and Fig. S1). A more extensive species sampling within each transition will help us understand whether different covariance structures match the independent transitions to hummingbird pollination. However, the lack of significant phylogenetic signal suggests that sister species do not necessarily have similar P-matrices. Accordingly with our results, the idea that pollinator specialization promotes the evolutionary convergence of floral traits has been supported before (e.g. Ortega-Olivencia *et al*. 2012, Rosas-Guerrero *et al*. 2014). Following a morphospace approximation, we found that flower size was the most conspicuous difference between bee- and hummingbird-pollinated species. This floral trait expresses huge variation among angiosperms (Krizek & Anderson 2013) and also plays a central role deterring or attracting different floral visitors (Castellanos *et al*., 2004; Cronk & Ojeda, 2008). Interestingly, size has been suggested as a genetic line of least resistance in other cases of adaptive radiation. For example, in New World monkeys diet diversification occurred through clear differences in skull size rather than on the phenotypic variance-covariance patterns (Marroig & Cheverud, 2005). Our results for *Salvia* flowers also support the idea that multivariate diversification (transition from bee to hummingbird pollination) occurred through the major axis of variation in flower size but also involved changes in **P**-matrix structure (see also Sosenski *et al*., 2010).

This article is protected by copyright. All rights reserved.

Despite the fact that interactions among floral traits have long been considered as a crucial functional feature affecting pollination success (Stebbins, 1970; Berg, 1960; Armbruster *et al*., 1999; Herrera *et al*., 2002; Fenster *et al*., 2005; Ordano *et al*., 2008; Fornoni *et al*., 2016), this idea remains almost unexplored. During the last decades, there has been an increasing interest in evaluating how combinations of floral traits are quantitatively organized (i.e., phenotypically integrated or modular) (Berg, 1960; Armbruster *et al*., 1999; Pérez-Barrales *et al*., 2007; Pérez *et al*., 2007; Conner & Lande, 2014; Fornoni *et al*., 2016) and whether patterns of phenotypic floral integration affect reproductive success (e.g., Ordano *et al*., 2008). Our results provide some insights about the evolution of variances and covariances among floral traits. First, proportional changes in matrix size accounted for a significant amount of variation among **P**-matrices (changes in the total amount of phenotypic variance) suggesting a role of drift (Roff, 2000; Jones *et al.*, 2003; Maubecín *et al.*, 2016). Second, simulations also suggested that variation among species in the magnitude of corolla integration occurred independently from the transition from bee to hummingbird pollination. Changes in phenotypic integration were more associated with modifications in the variances than on the covariances among traits. Hence, further work is needed to clarify if there is an association between proportionality and integration in covariance matrices. Finally, some differences in floral trait (co)variances between floral syndromes were present, but they accounted for a small portion of the differences among **P**-matrices.

To conclude, this work introduces the covariance space as a way to visualize evolutionary changes in **P**-matrix structure, as a tool to test the association between variance-covariance structure of complex phenotypic structures with ecological conditions during species diversification, and to explore the evolutionary causes and consequences of trait covariances. The comparison between mean and variance-covariance spaces can help in the understanding of the pace of evolution (i.e., to what extent the variance-covariance matrix

This article is protected by copyright. All rights reserved.

Accepted Article

behind functional modularity changes during species diversification). Our findings indicate that patterns of trait association indeed evolved during the transition from bee to hummingbird pollination. In contrast with what was observed among bee-pollinated species, the transition toward hummingbird pollination was characterized by a diversification of **P**-matrices structure. Overall, our results support the convergence expectation on mean trait values following the pollination syndrome hypothesis and suggest that the covariance structure of the corolla should not be viewed as a constraint, at least during the evolutionary transition from bee to hummingbird pollination in the genus *Salvia*.

ACKNOWLEDGEMENTS

Previous drafts of this manuscript were written during a sabbatical stay of XX in the XXXXXXXXX financed by XXXXXXX. Financial support was additionally provided by XXX to XX, XXXXX to XX, XX and XX, and by XXXXXX to XXX. We thank XXXXX and XXXXXX for constructive criticism and comments and two anonymous reviewers that improved the manuscript throughout the review process. XXXXX shared unpublished information about *Salvia cuspidata*.

CONFLICT OF INTEREST

Authors declare no conflicts of interest.

This article is protected by copyright. All rights reserved.

Accepted Article

Accepted Article

LITERATURE CITED

Adams, D.C. 2014. A Generalized K Statistic for Estimating Phylogenetic Signal from Shape and Other High-Dimensional Multivariate Data. *Syst. Biol.* **63**: 685–697.

Anderson, M.J. 2001. A new method for non-parametric multivariate analysis of variance. *Austral Ecol.* **26**: 32–46.

Andrade Machado, F., Gonçalves Zahn, T.M. & Marroig, G. 2018. Evolution of morphological integration in the skull of Carnivora (Mammalia): Changes in Canidae lead to increased evolutionary potential of facial traits. *Evolution* **72**: 1399–1419.

Armbruster, W.S., Di Stilio, V.S., Tuxill, J.D., Flores, T.C. & Velázquez Runk, J.L. 1999. Covariance and decoupling of floral and vegetative traits in nine neotropical plants: a re-evaluation of Berg's correlation-pleiades concept. *Am. J. Bot.* **86**: 39–55.

Armbruster, W.S., Pelabon, C., Bolstad, G.H. & Hansen, T.F. 2014. Integrated phenotypes: understanding trait covariation in plants and animals. *Philos. T. Roy. Soc. B* **369**: 20130245.

Benitez-Vieyra, S., Fornoni, J., Perez-Alquicira, J., Boege, K. & Dominguez, C.A. 2014. The evolution of signal-reward correlations in bee- and hummingbird-pollinated species of Salvia. *Proc. Roy. Soc. B.* **281**: 20132934.

Berg, R.L. 1960. The ecological significance of correlation pleiades. *Evolution* **14**: 171–180.

Bookstein, F.L. & Mitteroecker, P. 2014. Comparing covariance matrices by relative eigenanalysis, with applications to organismal biology. *Evol. Biol.* **41**: 336–350.

Castellanos, M.C., Wilson, P. & Thomson, J.D. 2004. "Anti-bee" and "pro-bird" changes during the evolution of hummingbird pollination in *Penstemon* flowers. *J. Evol. Biol.* **17**: 876–885.

This article is protected by copyright. All rights reserved.

Accepted Article

Chartier, M., Jabbour, F., Gerber, S., Mitteroecker, P., Sauquet, H., von Balthazar, M., *et al.* 2014. The floral morphospace - a modern comparative approach to study angiosperm evolution. *New Phytol.* **204**: 841–853.

Cheverud, J.M., Wagner, G.P. & Dow, M.M. 1989. Methods for the comparative analysis of variation patterns. *Syst. Zool.* **38**: 201–213.

Conner, J.K. & Lande, R. 2014. Raissa L. Berg's contributions to the study of phenotypic integration, with a professional biographical sketch. *Philos. T. Roy. Soc. B* **369**: 20130250.

Cronk, Q. & Ojeda, I. 2008. Bird-pollinated flowers in an evolutionary and molecular context. *J. Exp. Bot.* **59**: 715–727.

Delph, L.F., Steven, J.C., Anderson, I.A., Herlihy, C.R. & Brodie III, E.D. 2011. Elimination of a genetic correlation between sexes via artificial correlational selection: Breacking a between-sex genetic correlation. *Evolution* **65**: 2872–2880.

Esquerré, D., Sherratt, E. & Keogh, J.S. 2017. Evolution of extreme ontogenetic allometric diversity and heterochrony in pythons, a clade of giant and dwarf snakes. *Evolution* **71**: 2829–2844.

Fenster, C.B., Armbruster, W.S., Wilson, P., Dudash, M.R. & Thomson, J.D. 2004. Pollination syndromes and floral specialization. *Annu. Rev. Ecol. Syst.* **35**: 375–403.

Fenster, C.B., Reynolds, R.J., Williams, C.W., Makowsky, R. & Dudash, M.R. 2015. Quantifying hummingbird preference for floral trait combinations: The role of selection on trait interactions in the evolution of pollination syndromes. *Evolution* **69**: 1113–1127.

Fornoni, J., Ordano, M., Pérez-Ishiwara, R., Boege, K. & Domínguez, C.A. 2016. A comparison of floral integration between selfing and outcrossing species: a meta-analysis. *Ann. Bot.* **117**: 299–306.

This article is protected by copyright. All rights reserved.

Accepted Article

Fragoso-Martínez, I., Martínez-Gordillo, M., Salazar, G.A., Sazatornil, F., Jenks, A.A., Peña, M. del R.G., *et al.* 2018. Phylogeny of the Neotropical sages (*Salvia* subg. Calosphace; Lamiaceae) and insights into pollinator and area shifts. *Plant. Syst. Evol.* **304**: 43–55.

Futuyma, D.J. 2010. Evolutionary constraint and ecological consequences. *Evolution* **64**: 1865–1884.

González, A.V., Murúa, M.M. & Pérez, F. 2015. Floral integration and pollinator diversity in the generalized plant-pollinator system of *Alstroemeria ligtu* (Alstroemeriaceae). *Evol. Ecol.* **29**: 63–75.

Goolsby, E.W. 2015. Phylogenetic comparative methods for evaluating the evolutionary history of function-valued traits. *Syst. Biol.* **64**: 568-578.

Goswami, A. 2006. Cranial modularity shifts during mammalian evolution. *Am. Nat.* **168**: 270–280.

Goswami, A., Smaers, J.B., Soligo, C. & Polly, P.D. 2014. The macroevolutionary consequences of phenotypic integration: from development to deep time. *Phil. T. Roy. Soc. B.* **369**: 20130254–20130254.

Gould, S.J. 2002. *The structure of evolutionary theory*. Harvard University Press, Cambridge.

Grabowski, M. & Porto, A. 2016. How many more? Sample size determination in studies of morphological integration and evolvability. *Methods Ecol. Evol.* **8**: 592–603.

Harmon, L.J. & Glor, R.E. 2010. Poor statistical performance of the Mantel test in phylogenetic comparative analyses. *Evolution* **64**: 2173–2178.

Harmon, L.J., Weir, T.J., Brock, C.D., Glor, R.E. & Challenger, W. 2008. GEIGER: investigating evolutionary radiations. *Bioinformatics* **24**:129-131.

Herrera, C.M. 2009. *Multiplicity in unity: plant subindividual variation and interactions with animals*. University of Chicago Press, Chicago.

Huxley, J.S. 1932. *Problems of relative growth*. Methuen & Company Ld., London.

This article is protected by copyright. All rights reserved.

Accepted Article

Jamniczky, H.A., Barry, T.N. & Rogers, S.M. 2015. Eco-evo-devo in the study of adaptive divergence: Examples from threespine stickleback (*Gasterosteus aculeatus*). *Integr. Comp. Biol.* **55**: 166–178.

Jones, A.G., Arnold, S.J. & Bürger, R. 2003. Stability of the G-matrix in a population experiencing pleitropic mutation, stabilizing selection, and genetic drift. *Evolution* **57**: 1747–1760.

Krizek, B.A. & Anderson, J.T. 2013. Control of flower size. *J. Exp. Bot.* **64**: 1427–1437.

Lázaro, A. & Santamaría, L. 2016. Flower-visitor selection on floral integration in three contrasting populations of *Lonicera implexa*. *Am. J. Bot.* **103**: 325–336.

Lewontin, R.C. 1966. On the measurement of relative variability. *Syst. Zool.* **15**: 141–142.

Manly, B.F.J. 2005. *Multivariate Statistical Methods: A primer*. Chapman and Hall, New York.

Mantel, N. 1967. The detection of disease clustering and a generalized regression approach. *Cancer Res.* **27**:209–220.

Marroig, G. & Cheverud, J.M. 2005. Size as a line of least evolutionary resistance: Diet and adaptive morphological radiation in New World monkeys. *Evolution* **59**: 1128–1142.

Maubecín, C.C., Cosacov, A., Sérsic, A.N., Fornoni, J. & Benitez-Vieyra, S. 2016. Drift effects on the multivariate floral phenotype of *Calceolaria polyrhiza* during a post-glacial expansion in Patagonia. *J. Evol. Biol.* **29**: 1523–1534.

Maynard-Smith, J., Burian, R., Kauffman, S., Alberch, P., Campbell, J., Goodwin, B., *et al.* 1985. Developmental constraints and evolution: A perspective from the Mountain Lake Conference on Development and Evolution. *Q. Rev. Biol.* **60**: 265–287.

Melo, D., Garcia, G., Hubbe, A., Assis, A.P. & Marroig, G. 2016. EvolQG - An R package for evolutionary quantitative genetics. *F1000Research* **4**: 925.

This article is protected by copyright. All rights reserved.

Accepted Article

Merilä, J. & Björklund, M. 2004. Phenotypic integration as a constraint and adaptation. In: *Phenotypic Integration: Studying the Ecology and Evolution of Complex Phenotypes* (M. Pigliucci & K. Preston, eds.), pp. 107–129. Oxford University Press, Oxford.

Mitteroecker, P. & Bookstein, F. 2009. The Ontogenetic Trajectory of the Phenotypic Covariance Matrix, with Examples from Craniofacial Shape in Rats and Humans. *Evolution* **63**: 727–737.

Murren, C.J. 2012. The integrated phenotype. *Integr. Comp. Biol.* **52**: 64–76.

Oksanen, J., Blanchet, F.G., Friendly, M., Kindt, R., Legendre, P., McGlinn, D., *et al.* 2017. *vegan: Community Ecology Package*. https://CRAN.R-project.org/package=vegan

Ordano, M., Fornoni, J., Boege, K. & Domínguez, C.A. 2008. The adaptive value of phenotypic floral integration. *New Phytol.* **179**: 1183–1192.

Ortega-Olivencia, A., Rodríguez-Riaño, T., Pérez-Bote, J.L., López, J., Mayo, C., Valtueña, F.J., *et al.* 2012. Insects, birds and lizards as pollinators of the largest-flowered Scrophularia of Europe and Macaronesia. *Ann. Bot.* **109**: 153–167.

Pavlicev, M., Cheverud, J.M. & Wagner, G.P. 2009. Measuring morphological integration using eigenvalue variance. *Evol. Biol.* **36**: 157–170.

Pelé, J., Becu, J-M., Abdi, H. & Chabbert, M. 2012. bios2mds: From BIOlogical Sequences to MultiDimensional Scaling. R package version 1.2.2. `https://CRAN.R-project.org/package=bios2mds`

Pérez-Barrales, R., Arroyo, J. & Scott Armbruster, W. 2007. Differences in pollinator faunas may generate geographic differences in floral morphology and integration in *Narcissus papyraceus* (Amaryllidaceae). *Oikos* **116**: 1904–1918.

Pérez-Barrales, R., Simon-Porcar, V.I., Santos-Gally, R. & Arroyo, J. 2014. Phenotypic integration in style dimorphic daffodils (Narcissus, Amaryllidaceae) with different pollinators. *Philos. T. Roy. Soc. B.* **369**: 20130258.

This article is protected by copyright. All rights reserved.

Phillips, P.C. & Arnold, S.J. 1999. Hierarchical comparison of genetic variance-covariance matrices. I. Using the Flury hierarchy. *Evolution* **53**: 1506–1515.

Revell, L.J. 2009. Size-correction and principal components for interspecific comparative studies. *Evolution* **63**: 3258–3268.

Reiss, K.Z. 2001. Using phylogenies to study convergence: The case of the ant-eating mammals. *Amer. Zool.* **41**: 507-525.

Roff, D. 2000. The evolution of the G matrix: selection or drift? *Heredity* **84**: 135.

Rosas-Guerrero, V., Aguilar, R., Martén-Rodríguez, S., Ashworth, L., Lopezaraiza-Mikel, M., Bastida, J.M., *et al.* 2014. A quantitative review of pollination syndromes: do floral traits predict effective pollinators? *Ecol. Lett.* **17**: 388–400.

Rosas-Guerrero, V., Quesada, M., Armbruster, W.S., Pérez-Barrales, R. & Smith, S.D. 2011. Influence of pollination specialization and breeding system on floral integration and phenotypic variation in *Ipomoea*. *Evolution* **65**: 350–364.

Schluter, D. 1996. Adaptive radiation along genetic lines of least resistance. *Evolution* **50**: 1766–1774.

Schwenk, K. & Wagner, G.P. 2004. The relativism of constraints on phenotypic evolution. In: *Phenotypic integration: studying the ecology and evolution of complex phenotypes* (M. Pigliucci & K. Preston, eds), pp. 390–408, Oxford University Press, Oxford.

Smith, K.L., Harmon, L.J., Shoo, L.P. & Melville, J. 2010. Evidence of constrained phenotypic evolution in a cryptic species complex of agamid lizards. *Evolution* **65**: 976–992.

Sosenski, P., Fornoni, J., Molina-Freaner, F.E., Weller, S.G. & Domínguez, C.A. 2010. Changes in sexual organ reciprocity and phenotypic floral integration during the tristyly-distyly transition in Oxalis alpina. *New Phytol.* **185**: 829–840.

This article is protected by copyright. All rights reserved.

Accepted Article

Stebbins, G.L. 1970. Adaptive radiation of reproductive characteristics in angiosperms: I Pollination mechanisms. *Annu. Rev. Ecol. Syst.* **1**: 307–326.

Steppan, S.J. 1997. Phylogenetic analysis of phenotypic covariance structure. I. Contrasting results from matrix correlation and common principal component analysis. *Evolution* **51**: 571–586.

Steppan, S.J., Phillips, P.C. & Houle, D. 2002. Comparative quantitative genetics: evolution of the G matrix. *Trends Ecol. Evol.* **17**: 320–327.

Strelin, M.M., Benitez- Vieyra, S., Fornoni, J., Klingenberg, C.P. & Cocucci, A. 2018. The evolution of floral ontogenetic allometry in the Andean genus *Caiophora* (Loasaceae, subfam. Loasoideae). *Evol. Dev.* **20**: 29–39.

Wagner, G.P. 1984. On the eigenvalue distribution of genetic and phenotypic dispersion matrices: evidence for a nonrandom organization of quantitative character variation. *J. Math. Biol.* **21**: 77–95.

Wagner, G.P. & Altenberg, L. 1996. Complex adaptations and the evolution of evolvability. *Evolution* **50**: 967–976.

Walker, J.B., Sytsma, K.J., Treutlein, J. & Wink, M. 2004. *Salvia* (Lamiaceae) is not monophyletic: implications for the systematics, radiation, and ecological specializations of *Salvia* and tribe Mentheae. *Am. J. Bot.* **91**: 1115–1125.

Walter, G.M., Aguirre, J.D., Blows, M.W. & Ortiz-Barrientos, D. 2018. Evolution of genetic variance during adaptive radiation. *Am. Nat.* **191**: E108–E128.

Watson, R.A., Wagner, G.P., Pavlicev, M., Weinreich, D.M. & Mills, R. 2014. The evolution of phenotypic correlations and "developmental memory". *Evolution* **68**: 1124–1138.

Wessinger, C.A. & Hileman, L.C. 2016. Accessibility, constraint, and repetition in adaptive floral evolution. *Dev. Biol.* **419**: 175–183.

This article is protected by copyright. All rights reserved.

Wester, P. & Claßen-Bockhoff, R. 2011. Pollination syndromes of New World *Salvia* species with special reference to bird pollination. *Ann. Mo. Bot. Gard.* **98**: 101–155.

Young, R.L. & Badyaev, A.V. 2006. Evolutionary persistence of phenotypic integration: influence of developmental and functional relationships on complex trait evolution. *Evolution* **60**: 1291–1299.

TABLES

Table 1. Loadings for a phylogenetic principal component analysis on log-transformed variables.

Trait	**PC1**	**PC2**
Lower lip length	0.305	-0.446
Lower lip width	0.104	-0.448
Upper lip length	0.548	-0.168
Upper lip width	0.439	-0.128
Corolla tube length	0.485	0.742
Corolla tube width	0.409	-0.072

This article is protected by copyright. All rights reserved.

Table 2. AIC values from Common Principal Component analyses comparing 18 species of *Salvia.* Numbers in bold correspond to the best model. Numbers in parentheses after CPC in the first column indicate the number of *i* principal components in common (*i* ranging from *n*-2 to 1, where *n* is the number of traits).

Model	All species (n = 18)	Hummingbird - pollinated species (n = 8)	Bee-pollinated species (n = 10)
Equality	1037.655	472.195	448.444
Proportionality	876.896	368.254	396.103
CPC	752.483	315.452	**357.249**
CPC (4)	760.212	316.534	367.378
CPC (3)	784.806	328.513	380.800
CPC (2)	775.369	323.762	367.341
CPC (1)	757.678	331.857	370.089
Unrelated	**714.000**	**294.000**	378.000

FIGURE CAPTIONS

Figure 1. Measured traits and examples of *Salvia* flowers. a) Measured corolla traits in lateral (top) and frontal (bottom) views of a *Salvia* flower. CTL, corolla-tube length; CTW, corolla-tube width; LLL, corolla lower lip length; LLW, corolla lower lip width; ULL, corolla upper lip length; ULW, corolla upper lip width. b) Flower of *Salvia fulgens*, a hummingbird-pollinated species. c) Flowers of *Salvia cuspidata* ssp. *gilliesii*, a bee-pollinated species.

Figure 2. Mean trait morphospace constructed with six corolla traits from 18 *Salvia* species obtained after a Phylogenetic Principal Component Analysis. Red dots indicate hummingbird-pollinated *Salvia* species, while blue dots correspond to bee-pollinated species. The same shade colours indicate the convex hulls.

This article is protected by copyright. All rights reserved.

Accepted Article

Figure 3. Covariance space of corolla traits in 18 *Salvia* species. a) Left: First three principal coordinates of the covariance space. Red dots indicate **P**-matrices from hummingbird-pollinated species, while blue dots correspond to **P**-matrices from bee-pollinated species. The same colours indicate the convex hulls. Right: Pearson correlations between the principal coordinates and the variances and covariances of the **P**-matrices. Names follow the convention of Figure 1, *e.g* lll-lll indicate the variance in lower lip length and lll-ctl is the covariance between lower lip length and corolla tube length.

Figure 4. Projection of simulated matrices into the **P**-matrix space. a) Arrows indicate changes in proportionality inside the **P**-matrix space. The start of the arrow corresponds to a matrix having half the total variance as the original matrix. The end of the arrow corresponds to a matrix having double the total variance as the original matrix. b) Arrows indicate changes in phenotypic integration inside the **P**-matrix space. The start of the arrow corresponds to a matrix where the first eigenvector accounts for 25% of the total variance. The end of the arrow corresponds to a matrix where the first eigenvector accounts for 85% of the total variance.

This article is protected by copyright. All rights reserved.

Accepted Article

Accepted Article

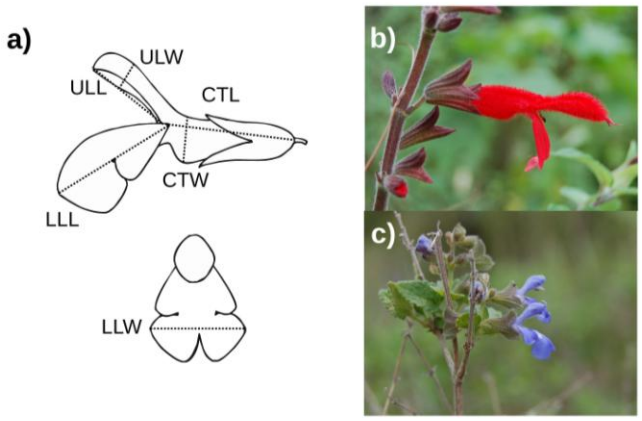

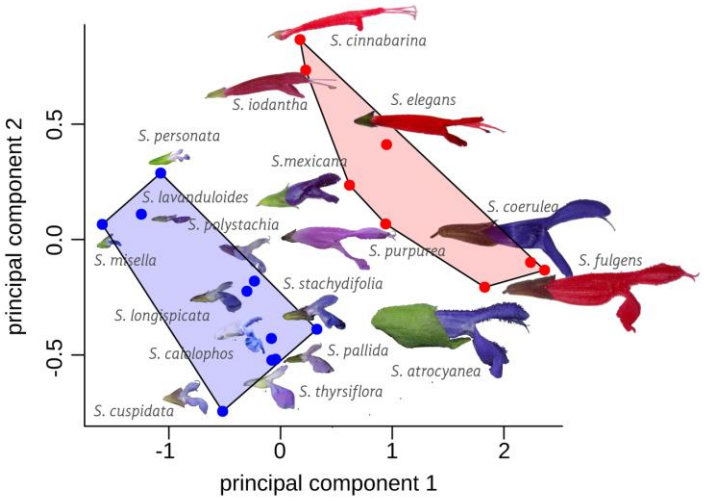

This article is protected by copyright. All rights reserved.

Accepted Article

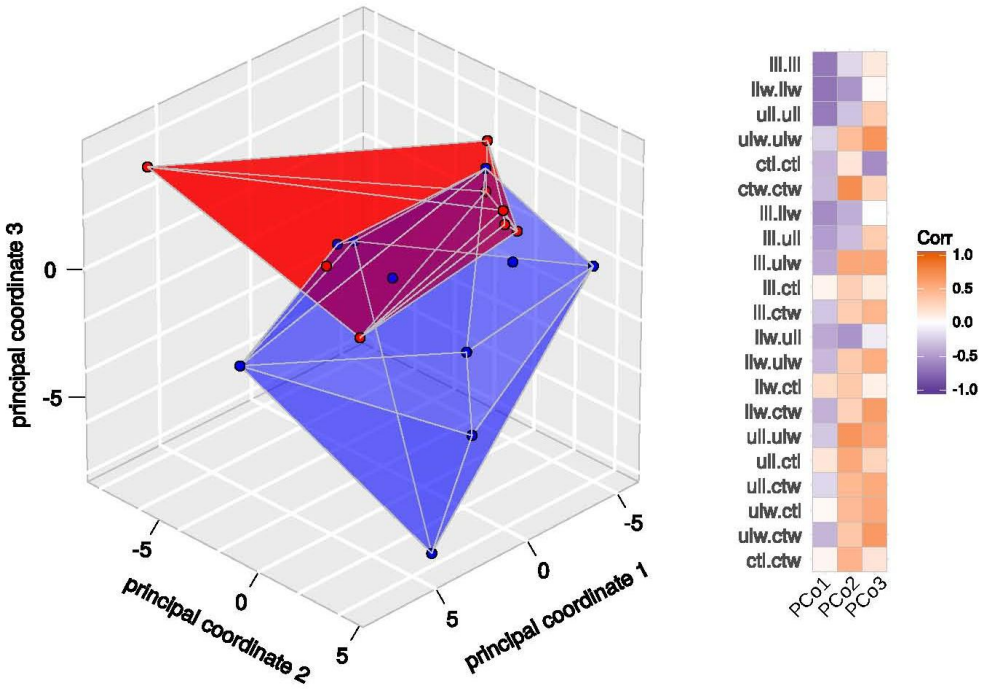

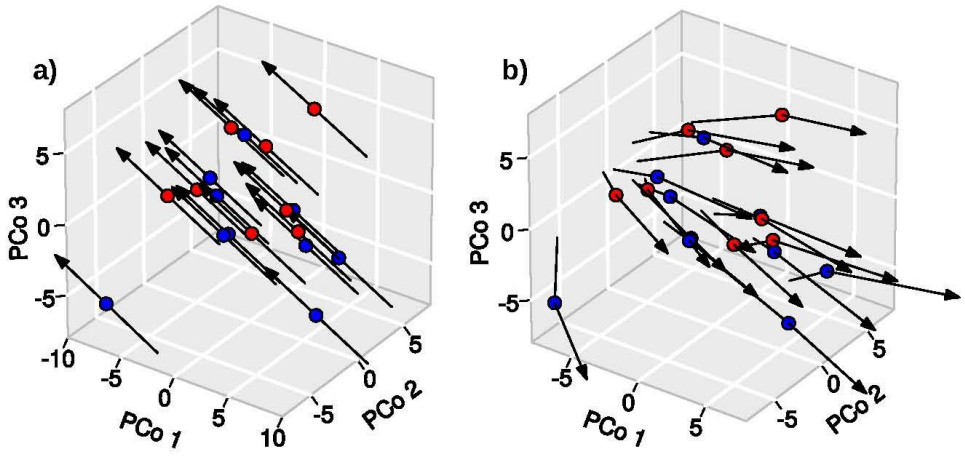

This article is protected by copyright. All rights reserved.